

8.2 Numerical Study of Relationships between Convective Vertical Velocity, Radar Reflectivity Profiles, and Passive Microwave Brightness Temperatures

Yaping Li, Edward J. Zipser, Steven K. Krueger, and Mike A. Zulauf

University of Utah, Salt Lake City, UT

1. INTRODUCTION

Numerous studies (e.g., Nesbitt et al. 2000; Toracinta et al. 2002) have used the Tropical Rain Measuring Mission (TRMM) proxy variables [i.e., TRMM Precipitation Radar (PR) and Microwave Imager (TMI) data] to examine regional and global distribution of “convective intensity”. The use of the TRMM observations to represent convective vertical velocity, probably the most appropriate measure of convective intensity, is by inference, relying on a simple conceptual model: a convective system, with larger radar reflectivity reaching higher height level and lower brightness temperature, is expected to have a convective core with greater updraft speed. However, even if this simple conceptual model is correct, it does not describe any functional relationship. In an attempt to make the conceptual model more quantitative, this study employs the 3-D University of Utah (UU) Cloud-Resolving Model (CRM) to simulate convective systems during the Kwajalein Experiment (KWAJEX).

2. KWAJEX

The Kwajalein Experiment (KWAJEX) centered on Kwajalein Atoll in the Republic of the Marshall Islands took place during the period 23 July-15 September 1999, which was one of several field campaigns as part of the NASA TRMM ground validation program and designed to address particular issues related to the remote measurements made by the TRMM satellite (Yuter et al. 2005). During the 55 project days, isolated convective systems of small horizontal dimension were prevalent (Cetrone and Houze 2005). Three of the days included broad MCSs that moved through the KWAJEX domain (25-26 July, 11-12 August, and 2-3 September). In this study, the large mesoscale convective system (MCS) of 11-12 August, which is the best-sampled MCS during the KWAJEX, is simulated.

3. MODEL AND EXPERIMENT DESIGN

The 3-D UU CRM has been described in detail in Zulauf (2001). The model is based upon a nonhydrostatic set of primitive equations. The quasi-compressible approximation is used, in which the speed of sound is artificially reduced. This model is specifically designed to examine small-scale atmospheric flows. The microphysical scheme is the Krueger et al. (1995) modification of the single moment, 3-ice microphysics parameterization scheme first developed by Lin et al. (1983) and Lord et al. (1984). It features five classes of hydrometeors (cloud liquid water, cloud ice, rain, snow and graupel), and assumes monodisperse distributions for the non-precipitating cloud water and cloud ice and inverse exponential size distributions for the precipitating hydrometeors, rain, snow and graupel. The scheme predicts the evolution of the mixing ratios of each species.

The simulation employs a grid of $128 \times 128 \times 80$ points with a horizontal grid size of 500 m and a variable vertical grid size that increases from 75 meters at the surface to 600 m at the top of the domain (at 27 km). It is initialized using the observed sounding at 0000 UTC 10 August and driven by the time-varying large-scale forcing, taken from the objectively analyzed dataset, based on the observations made over the Kwajalein area during the KWAJEX IOP from July 24 to September 14, 1999 and generated using the multivariate constrained optimization method of Zhang et al. 2001. The domain-averaged horizontal wind profile is nudged to the observed horizontal wind profile on a 2-h timescale. The time-varying radiative heating rate profile is calculated using Q. Fu's radiation code. The surface latent and sensible fluxes have been prescribed in the simulations. Periodic lateral boundary conditions are used. This is consistent with imposing horizontally uniform large-scale forcing. The simulation is run for 72 hours starting at 0000 UTC of August 10th, 1999. Only the 12 hour period between 1800 UTC of August 11th and 0600 UTC of August 12th 1999 is analyzed in this study.

* Corresponding author address: Yaping Li, Univ. of Utah, Department of Meteorology, Salt Lake City, UT 84112
e-mail: yaping@met.utah.edu.

4. RESULTS

4.1 Identify Simulated Precipitation Features

The simulated brightness temperatures (Tbs) are computed using modeled hydrometeor fields as input to a microwave radiative transfer model (Kummerow and Weinman 1988). Simulated radar reflectivity is calculated using the relations of Smith et al. (1975) and Smith (1984). The simulated Tb and reflectivity are convolved from model grid size of 500 m to TRMM TMI and PR resolution, respectively. Based on the contour plots of convolved simulated 85-GHz brightness temperature and radar reflectivity, the simulated precipitation features are defined in a way that is consistent with the way used to analyze the TRMM data in Nesbitt et al. 2000, i.e., an area is required to be 300 or more contiguous grids in size ($\sim 75 \text{ km}^2$; model with a horizontal grid size of 0.5 km and a grid area of 0.25 km^2) and to contain either a near-surface reflectivity $\geq 20 \text{ dBZ}$ or an 85 GHz brightness temperature $\leq 250 \text{ K}$. For the total forty-nine snapshots (15 minute time-step) during the 12-hour simulation period, there are 66 precipitation features identified, 35 of which are satisfy the criteria for PF with MCS in Nesbitt et al. 2000 [area $> 2000 \text{ km}^2$ (8000 or more contiguous grids) with a minimum brightness temperature $< 225 \text{ K}$].

4.2 Relationship Between Simulated Convective Vertical Velocity, Microwave Brightness Temperature, and Radar Reflectivity

The animation of x-y plots of simulated maximum vertical velocity, maximum radar reflectivity in each model column, and 85-, 37-GHz brightness temperatures for the 12-hour period (not shown) indicates that large vertical velocity is highly correlated with high radar reflectivity and low microwave brightness temperatures. Figure 1 shows one example of the x-y plots of vertical velocity, radar reflectivity, and 85-, 37-GHz brightness temperature. At this moment, the centers of high reflectivity ($> 40 \text{ dBZ}$) are highly correlated with large vertical velocity centers ($w > 10 \text{ m/s}$). The centers of 85- and 37-GHz brightness temperatures are well correlated with large vertical velocity centers too. All these show that radar reflectivity and microwave brightness temperatures are strongly dependent on convective vertical velocity.

In order to get some quantitative relationship between these quantities, the maximum vertical velocity, the minimum 85- and 37-GHz brightness

temperatures, the maximum reflectivity at 6- and 9-km, and the maximum height of the 20- and 40-dBZ echo are analyzed for each simulated precipitation feature. Then, the correlations between vertical velocity, microwave brightness temperature, and radar reflectivity are analyzed based on the analysis of simulated precipitation features.

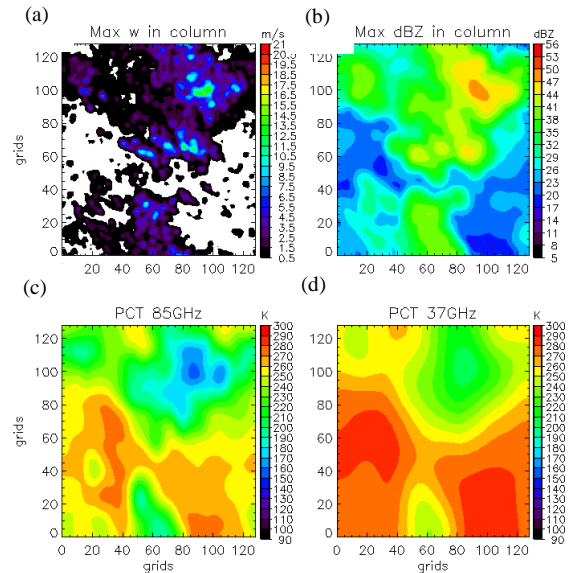


Figure 1. X-Y plots of simulated (a) maximum vertical velocity in model columns; (b) maximum radar reflectivity in model columns; (c) 85-GHz; (d) 37-GHz brightness temperature at the snapshot of 0015 UTC on August 12 1999.

In order to get some quantitative relationship between these quantities, the maximum vertical velocity, the minimum 85- and 37-GHz brightness temperatures, the maximum radar reflectivity at 6- and 9-km, and the maximum height of the 20- and 40-dBZ echo are analyzed for each simulated precipitation feature. Then, the correlations between vertical velocity, microwave brightness temperature, and radar reflectivity are analyzed based on the analysis of simulated precipitation features.

Radar reflectivity and microwave brightness temperature are associated with ice water path, therefore, the correlation between simulated maximum vertical velocities and maximum ice water paths (graupel + snow + cloud ice) in the simulated precipitation features is analyzed first (Figure 2a). There is a positive correlation between maximum vertical velocity and maximum ice water path, with some scatter. The correlation coefficient R reaches 0.87. There are no points in the lower-right quadrant of the plot, indicating

that large ice water path cannot coexist with a weak updraft speed.

Figure 2b shows the correlation between minimum 85- and 37-GHz brightness temperatures for simulated precipitation features. Categorizing these precipitation features by vertical velocity (in different colors), features with lower minimum 85- and 37-GHz brightness temperatures tend to have higher vertical velocity. There is a positive correlation between minimum 85- and 37-GHz brightness temperatures, with a correlation coefficient of 0.92.

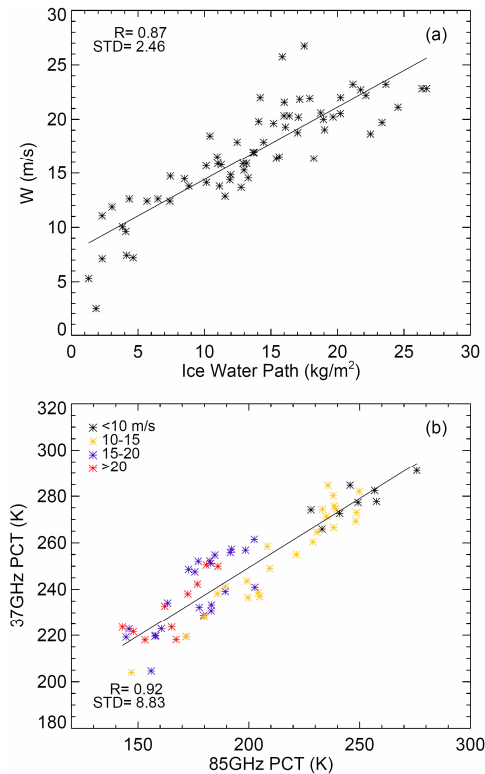


Figure 2. Correlation diagrams (a) between simulated maximum convective vertical velocity in column and ice water path; (b) between simulated 85- and 37-GHz brightness temperatures with vertical velocity categories. Asterisk in different color represents different convective vertical velocity category.

From Figure 3, the simulated minimum 85- and 37-GHz brightness temperatures have an almost negative linear relationship with vertical velocity. For 85-GHz brightness temperature, the correlation coefficient R reaches -0.83 , and the coefficient of -0.69 for 37-GHz PCT, which means that the lower minimum 37-, 85-GHz brightness temperatures are associated with higher convective vertical velocities.

The correlation diagrams between simulated radar reflectivity profiles and convective vertical velocity are shown in Figures 4 and 5. There is a good correlation between simulated maximum vertical velocity and radar reflectivity profiles: convective systems with higher radar reflectivities reaching upper levels tend to have stronger convective vertical velocities. From Figure 4, the correlation coefficients are separately 0.85 and 0.88 for the relationship of simulated maximum radar reflective at 6- and 9-km to the maximum convective vertical velocity, which implies that strong convective systems with large updraft velocities loft large ice particles into the mid- and upper troposphere.

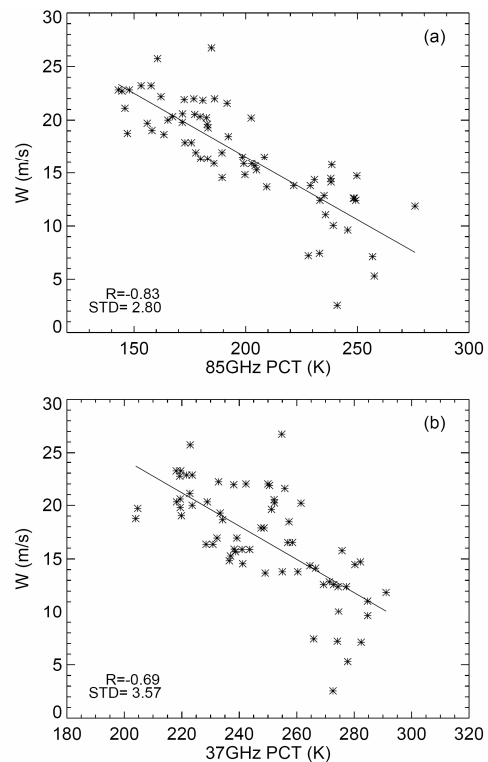


Figure 3. Correlation diagrams between simulated maximum convective vertical velocity and (a) minimum 85-GHz; (b) minimum 37-GHz brightness temperatures.

A positive relationship also shows up between the simulated maximum convective vertical velocity and maximum height of the 20- and 40-dBZ echo (Figure 5), though there is also much scatter, especially for the maximum height of the 40-dBZ echo. The correlation coefficients are 0.88 and 0.8, respectively. It is indicated again that large updraft speeds loft large ice particles into high levels.

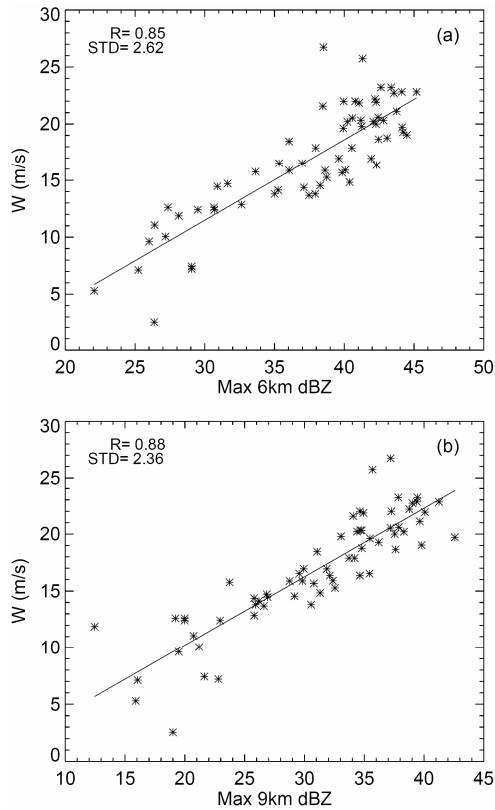


Figure 4. Correlation diagrams between simulated maximum convective vertical velocity and maximum reflectivity at (a) 6 km; (b) 9 km.

5. CONCLUSION

There is a good relationship between simulated convective vertical velocity, simulated radar reflectivity profiles and simulated microwave brightness temperatures at 85- and 37-GHz. A correlation coefficient of -0.83 and -0.69 is found between 85-, 37-GHz brightness temperature and updraft speed, respectively, which means the lower minimum 37- and 85-GHz brightness temperatures are associated with higher convective vertical velocities. Though there is also some scatter, there is a positive correlation between maximum vertical velocity and maximum radar reflectivity at 6- and 9-km, and maximum height of the 20- and 40-dBZ echo. The correlation coefficients are all greater than 0.8. The convective systems with stronger convective vertical velocity tend to be related to larger radar reflectivity at 6- and 9-km, higher maximum height of the 20- and 40-dBZ echo, and lower minimum 85- and 37-GHz brightness temperatures. *Statistically, the TRMM measurables are good proxies for convective intensity.*

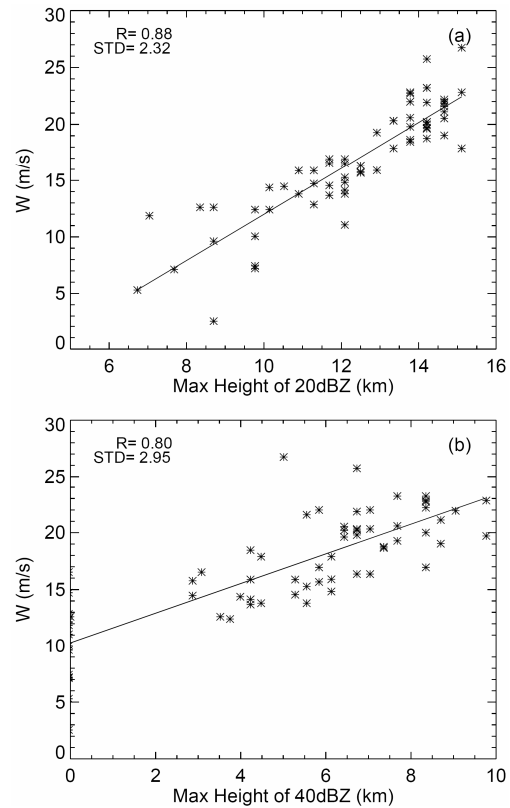


Figure 5. Correlation diagrams between simulated maximum convective vertical velocity and maximum height of the (a) 20 dBZ; (b) 40 dBZ echo.

REFERENCE

- Cetrone, J. and R. A. Houze Jr., 2006: Characteristics of Tropical Convection over the Ocean near Kwajalein. *Mon. Wea. Rev.*, **134**, 834–853.
- Krueger, S. K., Q. Fu, K. N. Liou, and H-N. S. Chin, 1995: Improvements of an ice-phase microphysics parameterization for use in numerical simulations of tropical convection. *J. Appl. Meteor.*, **34**, 281-287.
- Kummerow, C., and J. A. Weinman, 1988: Determining microwave brightness temperatures from horizontally finite, vertically structured clouds. *J. Geophys. Res.*, **93**, 3720-3728.
- Lin, Y. L., R. D. Farley, and H. D. Orville, 1983: Bulk parameterization of the snow field in a cloud model. *J. Climate Appl. Meteor.*, **22**, 1065-1092.

- Lord, S. J., H. E. Willoughby and J. M. Piotrowicz, 1984: Role of a parameterized ice-phase microphysics in an axisymmetric tropical cyclone model. *J. Atmos. Sci.*, **41**, 2836–2848.
- Nesbitt, S. W., E. J. Zipser, and D. J. Cecil, 2000: A census of precipitation features in the Tropics using TRMM: Radar, ice scattering, and lightning observations. *J. Climate*, **13**, 4087-4106.
- Smith, P. L., Jr., C. G. Myers and H. D. Orville, 1975: Radar reflectivity factor calculations in numerical cloud models using bulk parameterization of precipitation. *J. Appl. Meteor.*, **14**, 1156-1165.
- _____, 1984: Equivalent radar reflectivity factors for snow and ice particles. *J. Climate Appl. Meteor.*, **23**, 1258-1260.
- Toracinta, E. R., and E. J. Zipser, 2001: Lightning and SSM/I-ice-scattering mesoscale convective systems in the global tropics. *J. Appl. Meteor.*, **40**, 983-1002.
- Yuter, S. E., R. A. Houze Jr., E. A. Smith, T. T. Wilheit, and E. J. Zipser, 2005: Physical characterization of tropical oceanic convection observed in KWAJEX. *J. Appl. Meteor.*, **44**, 385-415.
- Zhang, M. H., J. L. Lin, R. T. Cederwall, J. J. Yio, and S. C. Xie, 2001: Objective analysis of ARM IOP data: Method and sensitivity. *Mon. Wea. Rev.*, **129**, 295–311.
- Zulauf, M. A., 2001: Modeling the effects of boundary layer circulations generated by cumulus convection and leads on large-scale surface fluxes. Ph.D. dissertation, Department of Meteorology, University of Utah, 177pp.